Pathloss Measurements and Modeling for UAVs Connected to Cellular Networks

Amorim, Rafhael Medeiros de; Mogensen, Preben Elgaard; Sørensen, Troels Bundgaard; Kovács, István ; Wigard, Jeroen

Published in:
2017 IEEE 85th Vehicular Technology Conference (VTC Spring)

DOI (link to publication from Publisher):
10.1109/VTCSpring.2017.8108204

Publication date:
2017

Document Version
Accepted author manuscript, peer reviewed version

Pathloss Measurements and Modeling for UAVs Connected to Cellular Networks

Rafhael Amorim, Preben Mogensen, Troels Sørensen
Department of Electronic Systems
Aalborg University, Denmark
{rma, pm, tbs}@es.aau.dk

István Z. Kovács, Jeroen Wigard
Nokia Bell Labs,
Aalborg, Denmark
{istvan.kovacs, jeroen.wigard}@nokia-bell-labs.com

***Abstract*—This paper analyzes the radio channel between cellular network and Unmanned Aerial Vehichles (UAVs). The assessment is done by means of field measurements performed in a rural environment in Denmark. The tests were conducted in an operating LTE network (800 MHz), using a commercial cell phone placed inside the frame of a winged UAV. Trials were conducted with UAV flying at 5 different heights measured above ground level (20, 40, 60, 80 and 100m) and a pathloss regression line was obtained from the results. Thereafter, an analysis of downlink (DL) interference is performed for the reported measurements, which suggests that there is a height-related degradation on signal-to-interference levels. Three possible sources for this effect are also presented and discussed in this paper: expanded radio horizon at higher levels, line-of-sight (LOS) clearing and decreased obstruction of the first Fresnel zone. The importance of a better quantification of these factors are stressed as future work plans are described.**

I. Introduction

UAVs, also known as drones, have a promising potential to reduce risk, cost, and time deployment for many activities, such as buildings inspection or search and rescue missions. Most of this potential is yet to be explored, as the operational range for drones is still very limited. The current policy of many air space agencies is to limit UAVs operational ranges in order to ensure a safe usage of the airspace, resulting in strict regulations imposed to drones users, such as the requirement of visual line of sight between controler and UAV during all phases of the flight. [1].

One important enabler for future UAV activities is the deployment of a reliable communication and control link (C2), also known as control and non-payload communications (CNPC). The C2 link will be responsible for exchanging all flight-related communication for beyond line-of-sight applications, such as telemetry, air traffic information and remote commands. Although the C2 link is considered to be deployed in dedicated frequencies by many [2], cellular networks may already be able to offer operating ground infrastructure that could make C2 links more cost efficient and ubiquitous, and might be considered as an alternative. Not only limited to supporting the C2 link, the cellular networks are also strong candidates to be in charge of payload information, such as real-time footage or other messages to be carried to/from drones.

Hence, the 3D pathloss modelling is an important topic to be regarded as it will enable simulation models and a better performance assessment for UAVs using cellular network resources. The challenges of this topic are addressed in this paper based on airborne measurements. Although there are several propagation models for typical cellular networks, their suitability for UAVs use case is yet to be proven since this propagation environment has its own specificities.

For ground users, radio waves propagating from base stations are subjected to phenomena as refraction, reflection and absortion caused by their interaction with buildings, trees, hills and other scattering objects present in the radio path between the transmitter and the receiver. In these scattering environments the signal is attenuated due to non line-of-sight propagation (NLOS). UAVs flying above rooftops and other obstructions are also subjected to these effects, but in a much smaller degree, while they also experience an increased likelihood of line-of-sight (LOS) transmissions.

On the other hand, by flying above the ground level, the UAV may observe an unobstructed path not only with the serving base station but also with many different interfering base stations in the same area. Because of this, assessments on interference levels for airborne UAVs are presented in this paper. It is worthy to mention that cellular networks are typically optimized for terrestrial usages which imposes some challeges to be discussed throughout this paper to their aerial usage.

A. Related Work

A significant contribution to this topic has been produced by the authors of [3] which have published a series of studies

Fig. 1. Cumulus One. UAV used for measurements

about air-to-ground (ATG) propagation channels based on measurements collected by large airbone UAVs. The measurements were performed in C-Band (5060 MHz) and L-Band (968 MHz), being both the bands pointed out by ITU (International Telecommunications Union) as main candidates for dedicated C2 links. In [3] the measurements are performed for over-the-water flights and the results show that due to the smooth water surface, the model that best fits the measuremens are the curved earth 2-Ray model (CE2R). The "lobbing" effect caused by the second ray is more apparent for distances above 10km, and is more prominent on L-Band data. Measurements performed in a hilly suburban environment shown the presence of additional multipath components, deviating from the simple 2-Ray model. Linear fits using freespace pathloss model (FSPL) on log scale show standard deviations between 3.2 and 3.6 dB in L-Band, which is a good fit when compared to the range of 6-10 dB often observed on terrestrial cellular pathloss measurements [4]

In [5], measurements in mountainous environments are fit using a log-distance model with pathloss coefficients between 1.6 and 1.8, slightly less than the FSPL value, which the authors attribute to some waveguiding observed on the valley region. Near-urban environment is investigated in [6] and the pathloss shows a pattern approximated by FSPL for the measured distances.

B. Paper Contributions and Organization

All the measurements cited in subsection I-A were taken on C-band and L-band empty bands, using a large UAV flying in heights around 500m-2km. This paper presents results collected in an operating LTE network at 800 MHz flying at current authorized heights for commercial UAVs (20-100m). It also presents assessmnet on the interference reported by the measurement device, regarding the cellular multicell environment. The final part of the paper is dedicated to a more detailed discussion about the challenges in obtaining a generic pathloss model, especially for interfering cells.

The paper is organized as follows: section II describe the measurements setup, while the results are discussed in section III. Then, a more detailed investigation in the height dependent factors that impact the propagation models for UAV-specific scenarios is presented in section IV. At last, future work planning and conclusions are presented, respectively, in sections V and VI.

II. Measurements Setup

On July 2016, measurements took place at a small airport in the vicinity of Odense, Denmark. The airport is mostly served by infrequent chartered flights which enabled the authorization for UAV flying activities.

For this study, a winged UAV (Cumulus One) was used to perform the flights (see Fig. 1). The cellular network data was collected by a regular cellular telephone (Samsung Galaxy S5), with the firmware adapted to allow the reading and reporting of radio measurements using Qualipoc software[1]. The cell phone was placed inside the UAV cavity, as depicted in Fig. 1. Henceforth in this paper, this mounting will be referred as UAV-UE. It is worth to note that, as the UE was in the inner part of the UAV-UE mounting, the sensitivity of the measurements was reduced due to the attenuation of the UAV frame. Pre-flight measurements were conducted to quantify this effect, and they indicated penetration losses around 10 dB.

The cellular phone was programmed to measure a 20 MHz LTE carrier, with center frequency around 810 MHz, and the phone's serving cell was locked to be the same during all flights (see Fig. 2). The selected cell is configured with 2-degrees electrical downtilt and is located at 22m height above the terrain. On average, at every 1s, the software recorded radio reports for the serving cell, including measurements like RSRP (reference symbol received power) and RSRQ (reference symbol received quality) [7].

The UE also reported some radio measurements for the neighbor cells. The number of neighbors and which neighbors are reported could not be defined in advance, as only cells discovered on each sampling interval were reported. For one cell to be detected, the UE must be capable of successfully separate its broadcast channel from the noise and interference power radiated by other adjacent cells. The power sensitivity for cell detection depends on the interference power at UE side: the heavier the interference, the higher the received power needs to be.

Once a cell is detected, the neighbor radio measurements are tagged with the physical layer cell identification (PCI) [8], which allows the mapping between them and their correspondent cells in operator's network. In LTE, there are 504 unique PCIs instances that can be attributed to the cells. Repetitions are managed by network planning to avoid neighbor cells to have the same PCI.

In the analysis presented in this paper, a circunference of 20km of radius around the landing zone was used as the search space for operator's cells. Reports collected by the UE were paired to cells in this region based on PCI numbers. The search area is limited to avoid ambiguity in cell mapping. Outliers samples whose PCI could not mapped within this area were discarded.

Antennas tilt and models were supplied by the network operator. Antennas radiation patterns and gains used in calculation were the same as provided by manufacturers datasheet. All transmitters have been assumed to have same wideband output power (49 dBm). Terrain altitude information was used to refine the calculation between base stations and the UAV-UE. The pathloss measurement was obtained from the difference between the transmitted power per received symbol (after applying antenna gains) and the RSRP. In order to mitigate the fast fading components in the measurements the collected samples were averaged by obtaining the local mean of samples

[1]More information about the Qualipoc software in https://www.rohdeschwarz. com/us/brochure-datasheet/qualipoc_android/

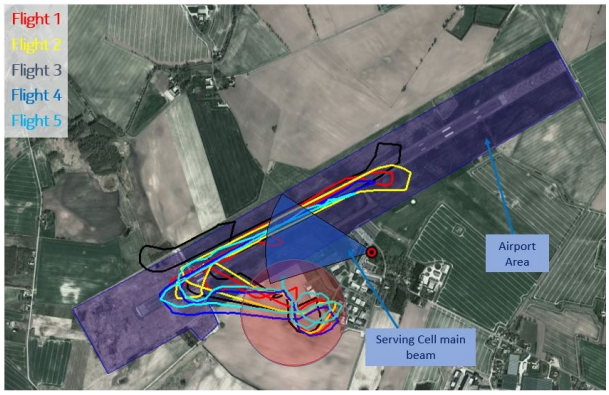

Fig. 2. Flight zone demarcation.

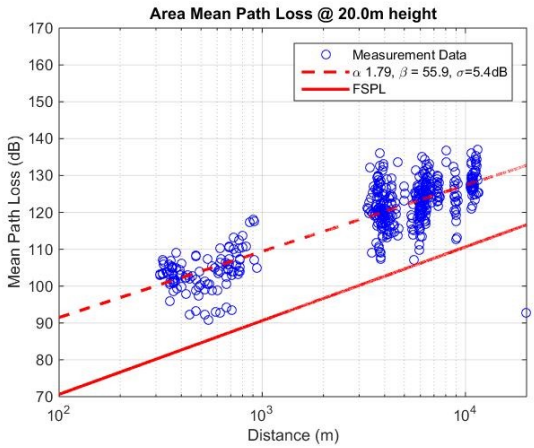

Fig. 3. Path Loss Measurements with UAV-UE

in windows of length equal to 40λ [9], where λ represents the radio wavelength.

Due to UAVs legislation in Denmark, flights were limited to visual line-of-sight range and at a max of 100m height. Therefore, all 5 flight routes performed were within such bounds, as depicted in Fig. 2. One of the goals of these measurements is to identify the effect of different heights on radio performance for the UAV-UE. Regarding this matter, in each measurement flight the controllers aimed at keeping the UAV-UE height as constant as possible. The flights heights, measured from ground level, followed an ascendant order with steps of 20m, i.e., the flight 1 was performed at 20m height, flight 2 was at 40m, and so on, up to flight 5, performed at 100m. To make the measurements comparable for these different heights the selected routes were similar for all 5 trials. The red circle on Fig. 2 represent the area used as taking off and landing zone for the UAV, therefore UAV heights are not stable within this zone. The data collected in this area was not considered in the analysis.

III. UAV-UE Measurements

A. Path Loss Modeling

Pathloss modeling was obtained by calculating the parameters α and β that best fit the measurements according to the log distance model widely used in previous literature [10]:

$$PL(d) = \beta + \alpha 10log_{10}(d) + X_0 \quad [dB] \tag{1}$$

where α accounts for the propagation coefficient (or pathloss exponent), β is a constant representing the close-in pathloss at a reference distance of 1m. X_0 is modelled as a random variable with Gaussian distribution, and zero mean and standard deviation σ, and represents the shadowing variation. In eq. 1, PL, β and X_0 are described in dB and d is in meters.

For the sake of example, the results for the flight performed at 20m height are shown in Fig. 3. The slope of the best fit line corresponds to α of 1.8, which is close to the exponent observed in freespace pathloss (FSPL), where $\alpha = 2$. The standard deviation of X_0 for this linear fit shows $\sigma = 5.4dB$. It is also possible to see in this figure, that due to the limitation on flight ranges for this campaign, there is a gap in the measurements for the range 1-4km, due to the absence of neighboring cells in this region that could be reported by the UE. Further tests are required to collect measurements that can fill this gap.

Even though the path loss exponent is below 2.0, there is an offset of approximately 20 dB between the collected samples and the reported measurements. This effect is probably related to an underestimation of the losses on the UAV fuselage. The pre-flight test was performed with the UAV-UE grounded, receiving the radio signal from its top part, while during the flights the arrival of the radio signals happened from the bottom or lateral parts of the UAV, which were reinforced to protect the phone inside the frame.

A summary with the results for all flight heights can be found in Table I. In all five flights the pathloss exponents are varying between 1.62 and 1.90, which are in line with the results presented for flight 1 and with values reported in [6]. and [11]. Although those values are below freespace propagation loss, it is important to remind that, by the own nature of the measurements, they are slightly biased downwards. It happens because the measurements are capped by the sensitivity threshold discussed in section II. This effect is also reinforced by penetration losses caused by UAV airframe, which causes an additional number of samples to be undetected, especially for the sites located further away from the flight region.

TABLE I
Log-distance fit

UAV-UE Height	α	σ [dB]	β [dB]	$\overline{SINR}$ [dB]	Median RSRP [dBm]
20 m	1.79	5.4	55.9	17.3	-85.2
40 m	1.69	4.9	57.6	11.9	-86.5
60 m	1.74	5.4	54.8	9.0	-87.3
80 m	1.62	5.8	59.7	6.2	-89.6
100 m	1.90	5.2	48.8	5.8	-87.9

B. UE DL SINR vs UAV Height

Onwards in this paper, the expression SINR (signal-to-noise plus interference-ratio) will be used to refer to downlink (DL) SINR. The values of the median SINR and RSRP collected in each flight are also shown in Table I. In this table, it is possible to see that as the UAV goes up, the value of the median SINR for the serving cell, $\overline{SINR}$, decreases. The SINR degraded 11.5 dB when UAV-UE moved up from 20m to 100m. It is expected some variation on the received signal power for the different heights, first because of changes in the elevation angle between base station and UAV-UE, and second because increments in the 3D distances caused by increasing the distance in the height dimension. However, no significant differences were identified in the median RSRP received from the serving cell, as reported in Table I. Therefore it is possible to infer there are stronger levels of interference for higher UAV-UE flights.

Another point worth to mention in Table I is that the steepest degradation on SINR was recorded in height elevation from 20m to 40m. From flight 1 to flight 2, degradation recorded was 5.4dB, and then 2.9, 2.8 and 0.4 dB in subsequent ones. It indicates that the interference increase is more prominent for lower heights, while it is subjected to smaller variation due to height gains at higher levels.

IV. SINR Degradation Causes

There are different factors that can cause the SINR degradation observed in previous section, and more measurements are needed in order to clarify how each of those factors impact final results, as related in section V. In this section, the main possible causes for this effect are presented in more details.

A. Expanded Horizon due to Earth curvature

Earth curvature imposes a limit on horizon range, which is the maximum straight path distance that do not intersect the planet's surface. Objects located beyond this range are not reachable in a straight path and are considered out of reach for optical communications.

For radio waves, the visual horizon may be expanded due to atmospheric effects. The dielectric constant of air varies with weather conditions and with height above ground. The height related variations cause eletromagnetic waves to bend as they were propagating in curved paths, keeping them closer to earth than they would be if travelling in a straight trajectory [4]. Approximating the Earth by a sphere of radius R, the radio horizon, D_{max}, between an UAV-UE and a base station with respective heights equal to $h_{ue} \ll R$, and $h_{bs} \ll R$, is by:

$$D_{max} \approx \sqrt{2kRh_{ue}} + \sqrt{2kRh_{bs}} \tag{2}$$

where k stands for the increase in radio range caused by atmospheric effects. Using the average value of $k = 4/3$ as suggested by ITU [12] for "standard" atmosphere conditions and assuming $R = 6370$ km, it is possible to simplify eq. 2 to:

$$D_{max} \approx 4.12 \left(\sqrt{h_{ue}} + \sqrt{h_{bs}} \right) \tag{3}$$

where D_{max} is represented in kilometers and h_{ue} and h_{bs} are in meters. So, assuming constant base station altitudes in the network, the range of distances where it can still interfere with UAV-UE received signals depends on the device altitude. As a consequence, the UAV at higher altitudes has an expanded radio horizon, which can add several different sources of interference. Under such assumptions and considering ground-reference at sea level, with $h_{bs} = 25m$, the radio horizon for UAV-UE for the flights heights of section II can be roughly approximated by the values presented in Table II. It is possible to see that the radio horizon of the signal expands from 39km at 20m to 62km at 100m, increasing the "reachable" area in 2300 km^2, potentially adding hundreds of new sources of interference. At some point, however, it is expected that the increases in interference power asymptotically approaches to zero, with the altitude as radio horizon becomes very large enough that pathloss atennuation makes the new interference sources negligible.

TABLE II
Theoretical Radio Horizon

$UAV - UEHeight(m)$	20	40	60	80	100
Radio Horizon (km)	39.0	46.6	52.5	57.5	61.8

B. LOS probability

Figure 4 shows how UAV height can impact the LOS clearing between network transmitters and the UAV-UE. In this figure, it is possible to see the altitude profile of the surface between a transmitter (Cell A), located close to the test area, and the UAV-UE. The surface profile includes buildings, trees and vegetations over terrain variation. The cell shown in this example corresponds to a sector where transmitter antenna is located at a height of 50 meters above ground level (19 meters of altitude). The UAV was placed in two different heights above ground - which is 16 meters of altitude at the landing zone - 20m and 40m. There is an obstruction to the line of sight between the network transmitter and the UAV at 20m height, probably caused by a building, which will cause attenuation to the transmitted signal. Once UAV moves up to 40 meters above ground in the same spot, there is no longer a LOS obstruction. Although this Cell's PCI was not identified by the UE in any measurements, the clearing of LOS would cause more interference power to be received by the UE.

In our measurement region, in South Denmark, the terrain is quasi-flat with no significant concentration of tall buildings in nearby cities. As so, the first meters above the ground correspond to the most significant gain in the LOS probability. The level of the first flight (20 m) probably see a very high gain compared to ground level, and future works must be done to test this hypothesis. Comparing the flight of the five trials described in section II, it is expected that the clearing of obstructions is more relevant factor between the first two

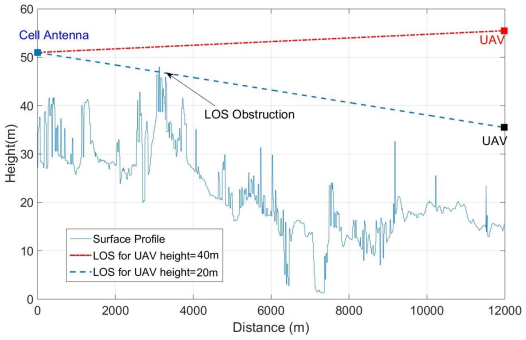

Fig. 4. LOS and surface profile interaction for Cell A

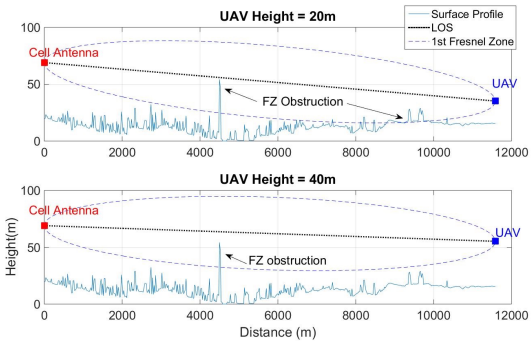

Fig. 5. Fresnel zone plots for Cell 2

(20m and 40m), which are the trials that presented the largest degradation in SINR according to the Table I. Above 40m, major part of cells in the neighboring region tend to be in LOS, and gains in line of sight probability with height become smaller

Freespace propagation for most neighbor sites within radio horizon ranges is an unrealistic assumption for most current cellular network deployments. For example, considering a pedestrian user, such as $h_{ue} = 1.5$, freespace assumption would correspond to paths remaining unobstructed for more than 20 km. But, in real urban and suburban scenarios, horizon are limited by buildings, vegetation, terrain elevations and other obstacles which make ranges usually fall to some hundreds meters.

Consequently, the interference component of SINR is usually dominated by a group of few neighbor cells, as the signal radiated by the others become severely attenuation before reaching the UE. For a flying UAV-UE, however, the presence of blocking surfaces become less likely, as it tends to be isolated from obstacles and other scattering surfaces. So, as the UAV-UE gains altitude, it is more likely it obtains clearing in LOS with several base stations, and some of those whose effect could be neglected for a pedestrian user, can become a source of significant interference power.

Consider $P[LOS|d, h_{ue}]$ to be the LOS probability between an UAV-UE, flying at a height h_{ue}, and a base station separated by a distance d. The value of $P[LOS|d, h_{ue}]$ is hard to estimate and depends significantly on scenario characteristics. In a mountainous area, such as rural Norway, it may require a higher h_{ue} to obtain clearing with neighbor base stations. For a dense urban area, e.g. Manhattan, the presence of tall buildings may limit gains $P[LOS|d, h_{ue}]$, for values of h_{ue} lower than dozens of meters, but it will go close to 1 after UAV-UE clears the tallest rooftops in the area.

C. Fresnel Zones Obstructions

In some cases, the existence of LOS between two devices is not sufficient to assure free space-like propagation. If the path travelled by the radio signal is partly obstructed, i.e. obstacles block the radio waves in the first Fresnel zone between transmitter and receiver, additional losses will incur. These diffraction losses can add as much as 6 dB on top of the free space loss. As a rule of thumb, obstructions $> 40\%$ of the first Fresnel zone can cause significant excess in pathloss when compared to freespace propagation [4].

The first Fresnel zone defines the region around the LOS path where the excess path length is between 0 and $\lambda/2$, where λ represents radio wavelength. The zone is defined by an ellipsoid around the signal main path, whose radius r_1, is given by:

$$r_1(d_0) = \sqrt{\frac{\lambda d_0 (D - d_0)}{D}}, \tag{4}$$

where D is the total distance between transmitter and receiver and d_0 is an intermediate distance, such as $d_0 \leq D$. The more obstructed is the Fresnel zone - in other words, the closer is the reflecting surface from the LOS path - the higher is the signal attenuation due to diffraction losses.

In Fig. 5, it is possible to see how elevations in UAV heights may clear the first Fresnel zone. The first Fresnel zone is plotted for the link between the UAV-UE in two different heights and one of the neighbor cells in the test area (Cell 2). For UAV height equal to 20m, there is a clear obstruction (probably caused by a building) for $d_0 = 4.5km$ that block a significant part of the Fresnel one(50%), which can potentially cause severe diffraction losses. Moreover, there is another important obstruction for d_0 between 8 and 10 km, caused by the radio signal intersecting with the Earth's surface. Once UAV moves up to 40 meters of height, the first obstruction blocks a smaller fraction of the Fresnel zone and the second obstruction caused by Earth's surface is not observed. The latter is specially important, because buildings landscape can vary significantly between two different points in the flight route, but variations on the surface of the Earth tend to be much smaller in this region.

V. Future Work

Airbore UAVs have degrees of freedom in the 3 dimensions, which introduce new variables to radio propagation modelling. Most common models used for cellular networks are usually adapted to pedestrian, vehicular and in-building users, and will

probably not produce realistic results when used for UAVs case.

A lot of uncertainties need to be unveiled in order to obtain a better model for UAVs flying at a given altitude, as evidenced by section IV. At first, it is necessary to quantify what are the most important factors to be considered in different scenarios and for different UAV heights. Then, it is important to obtain parameters that can be used to better describe the 3D propagation environment for UAVs. After analytical models are refined for UAVs case, network simulations can be performed enabling a more detailed study of network performance for such atypical users.

Under this scope, new tests are being envisioned for the near future. The new set of tests should be conducted over larger sampling distances (multiple flights), and in a different area. It is also being discussed the possibility of flying with a portable radio scanner, although it requires more planning due to the high payload that limit the options of drones to be used. If possible, the scanner would allow the lock of measurements in many different PCIs, which would produce more precise results in what concerns the potential causes for height related SINR degradation explored in this paper. Another possibility that could be explored in the future is the use of air gliders for measurements, what could expand the possibilities for the test setups.

VI. Conclusion

The set of cellular network measurements collected by the UAV-UE showed a pathloss slope that approximates freespace propagation for all five different heights measured. The measurement field was an open area with no obstructions between UAV and Base Station to cause significant signal attenuation, also no significant effect related to reflected paths were captured for the distances tested.

In all trials, measured values for pathloss slope are similar, with small variations caused by dynamic range limitation of measurement UE. However, it was observed a rembarkable SINR degradation between the lowest and highest flight levels. This result indicates the interference power increases with UAV-UE height. However, all neighbor cell measurements collected by UAV-UE show no power increase that could be accountable for the interference power increase.

Afterwards, a discussion on the challenges of obtaining a reliable path loss model for UAVs was presented, based on field measurements. Most part of uncertainties on pathloss modelling parameters for UAVs are height-related caused by changes on propagation environment. As it is pointed out, expanded radio horizon at higher altitudes, LOS likelihood and clearing of the first Fresnel zone are important radio factors that could observe significant variations within an area as a consequence of changes in UAV altitude. Future work is needed to quantify these effects in order to obtain a more realistic modelling for the propagation environment for UAVs.

Acknowledgment

The authors would like to thank UAS Danmark for the UAV used and for all support given during the measurements.

References

[1] EUROCONTROL, "Roadmap for the integration of civil Remotely-Piloted Aircraft Systems into the European Aviation System," 2013.

[2] FAA, "Integration of civil unmanned aircraft systems (uas) in the national airspace system (nas) roadmap," Tech. Rep., 2013.

[3] D. Matolak and R. Sun, "Air-ground channel characterization for unmanned aircraft systems - part i: Methods, measurements, and models for over-water settings," *IEEE Transactions on Vehicular Technology*, vol. PP, no. 99, pp. 1–1, 2016.

[4] J. Parsons, *The Mobile Radio Propagation Channel*. Wiley, 2000.

[5] R. Sun and D. W. Matolak, "Air-ground channel characterization for unmanned aircraft systems: The mountainous environment," in *2015 IEEE/AIAA 34th Digital Avionics Systems Conference (DASC)*, Sept 2015, pp. 5C2–1–5C2–9.

[6] D. W. Matolak and R. Sun, "Air-ground channel characterization for unmanned aircraft systems: The near-urban environment," in *Military Communications Conference, MILCOM 2015 - 2015 IEEE*, Oct 2015, pp. 1656–1660.

[7] " Evolved Universal Terrestrial Radio Access (E-UTRA); Physical Layer Measurements," 3GPP, Tech. Rep. TS 36.214 V8.7.0, September 2009.

[8] " Evolved Universal Terrestrial Radio Access (E-UTRA); Physical channels and modulation," 3GPP, Tech. Rep. TS 36.211 V8.9.0, December 2009.

[9] W. C. Y. Lee, "Estimate of local average power of a mobile radio signal," *IEEE Transactions on Vehicular Technology*, vol. 34, no. 1, pp. 22–27, Feb 1985.

[10] T. Rappaport, *Wireless Communications: Principles and Practice*, ser. Prentice Hall communications engineering and emerging technologies series. Prentice Hall PTR, 2002.

[11] D. W. Matolak and R. Sun, "Air-ground channel characterization for unmanned aircraft systems - part iii: The suburban and near-urban environments," *IEEE Transactions on Vehicular Technology*, vol. PP, no. 99, pp. 1–1, 2017.

[12] ITU-R, "Definitions of terms relating to propagation in non-ionized media," International Telecommunication Union, Recommendation P.310-9, Aug 1994.